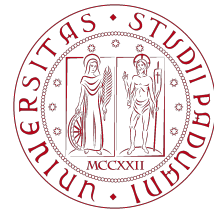


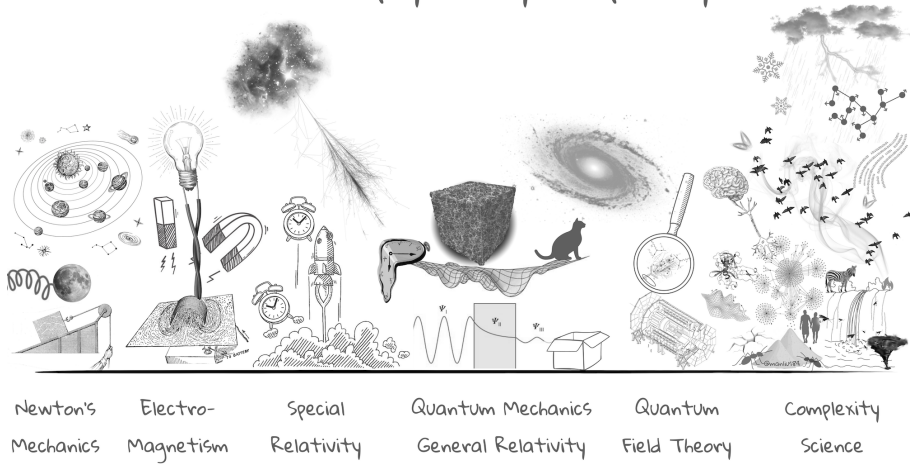
# Final Report

Physics of Complex Networks: Structure and Dynamics



UNIVERSITÀ  
DEGLI STUDI  
DI PADOVA

Areas of physics by complexity



## PoCN: Projects

Poccianti Gabriele

Last update: September 16, 2024

# Contents

---

<b>1 Swarmalators on a complete network</b>	<b>1</b>
1.1 Model presentation . . . . .	1
1.2 Numerical simulations . . . . .	2
1.3 Order Parameters . . . . .	4
1.4 ER Network . . . . .	5
<b>2 Modelling language competition on a complex network</b>	<b>7</b>
2.1 Model presentation . . . . .	7
2.2 Two-dimensional regular network . . . . .	8
2.3 Small-world Network . . . . .	9
<b>3 Social Connectedness Index I from Facebook</b>	<b>10</b>
3.1 Task Presentation . . . . .	10
3.2 Data Handling . . . . .	11
3.3 Data Analytics . . . . .	12
<b>4 Bibliography</b>	<b>14</b>

# 1 | Swarmalators on a complete network

---

## 1.1 | Model presentation

---

This model attempts to describe the simultaneous swarming (self-organization of positions in space) and synchronization (self-organization of internal states in time) observed in groups of animals. However, the resulting conclusions may also be applicable to other types of systems, such as colloidal suspensions of magnetic particles [1, 2, 3]. In many frameworks, those two behaviors—swarming and synchronization—interact. For instance some population of myxobacteria appear to have a biochemical degree of freedom (d.o.f.), which can be modeled as a phase. Evidence suggests the presence of a bidirectional coupling between spatial and phase dynamics [4]. Another example can be chemotactic oscillators, whose movements in space are mediated by the diffusion of a background chemical [5, 6].

In our treatment we considered a generalization of the Kuramoto model [7] on a network [8], where we ignored alignment (which would have required an additional d.o.f.), and we associated to each node at time  $t$  a phase and a position in the  $xy$  plane, as in [9, 10]:

$$\frac{d\mathbf{x}_i}{dt} = \mathbf{v}_i + \frac{1}{k_i} \sum_{j=1}^N A_{ij} \left[ \frac{\mathbf{x}_j - \mathbf{x}_i}{|\mathbf{x}_j - \mathbf{x}_i|} (A + J \cos(\theta_j - \theta_i)) - B \frac{\mathbf{x}_j - \mathbf{x}_i}{|\mathbf{x}_j - \mathbf{x}_i|^2} \right] \quad (1.1)$$

$$\frac{d\theta_i}{dt} = \omega_i + \frac{K}{k_i} \sum_{j=1}^N A_{ij} \frac{\sin(\theta_j - \theta_i)}{|\mathbf{x}_j - \mathbf{x}_i|} \quad (1.2)$$

$\mathbf{x}_i$ :	Position vector of the $i$ th swarmalator in space	$N$ :	Total number of swarmalators in the system
$\theta_i$ :	Phase of the $i$ th swarmalator	$J$ :	Position-phase coupling constant
$\mathbf{v}_i$ :	Self-propulsion velocity vector	$K$ :	Synchronization coupling constant
$\omega_i$ :	Natural frequency	$A$ :	Amplitude of the simple attraction term
$A_{ij}$ :	Element of the adjacency matrix of the network	$B$ :	Amplitude of the repulsion term
$k_i$ :	Degree of node $i$		

From now on we set

$$A = B = 1 \quad \mathbf{v}_i = \mathbf{0} \quad \omega_i = 0 \quad \forall i$$

We firstly considered a complete network and, by means of numerical simulations, we reproduced the different states of the system (described in [9, 10]) as  $J$  and  $K$  vary.

## 1.2 | Numerical simulations

For our simulation we relied on the R numerical implementation of the Kuramoto model showed in the third laboratory of this course (which used the deSolve package for numerical handling of ODEs). We extended the model including the equations of motion paying attention not to have singular initial conditions. Luckily [11] ensures that, given initial non-collisional data (initial phases and positions were uniformly generated in  $[0, 2\pi[ \times [0, 1]^2$ , with the previous prescription), a minimal inter-particle distance among the swarmalators is guaranteed. Even so we still checked the distance matrix at every step to prevent numerical divergence in eq. (1.1)-(1.2).

We chose the number of swarmalators  $N = 300$ , step of integration  $dt = 0.05$  and  $T = 2000$  timesteps (in fig. 1.5 more steps were necessary to reach the final configuration). We reproduced the noise-free states illustrated in fig 2 and fig 5 of [9]:

1. Static synchrony (fig. 1.2): the swarmalators form a circularly symmetric, crystal-like distribution in space, and are fully synchronized in phase.
2. Static asynchrony (fig. 1.3): at any given location  $\mathbf{x}$  all phases  $\theta$  can occur.
3. Static phase wave (fig. 1.4): since in this special case  $K = 0$  swarmalators' phases are frozen at their initial values. Still, since  $J > 0$ , units want to settle near others with similar phase.
4. Splintered phase wave (fig. 1.5): moving to  $K < 0$  static phase wave splinters into disconnected clusters of distinct phases where nodes execute small amplitude oscillations in position and phase.
5. Active phase wave (fig. 1.6): as  $K$  decreases oscillations increase in amplitude until swarmalators start to execute regular cycles in both space and phase <sup>1</sup>.

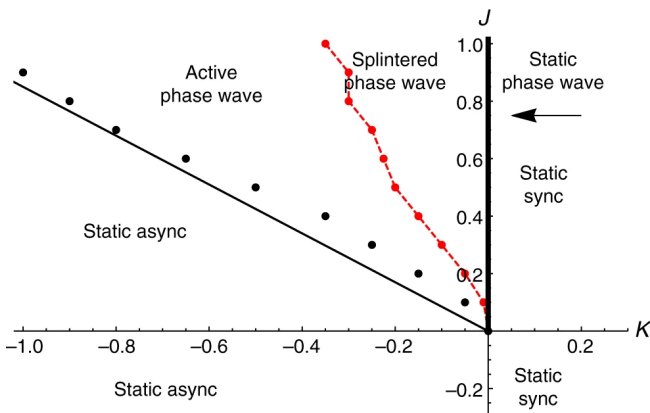


Figure 1.1: Phase diagram from [9]. The straight line separating the static async and active phase wave states is a semi-analytic approximation, while dots are derived from simulation data

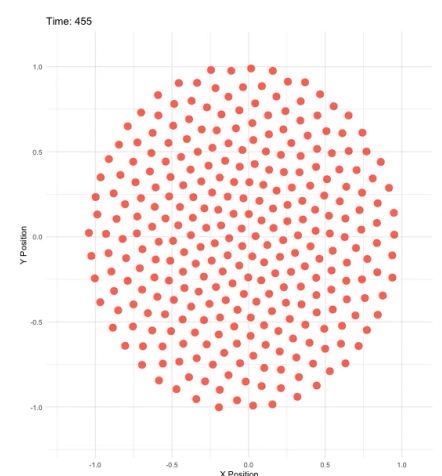


Figure 1.2: Static synchronous state ( $K = 1, J = 0.1$ )

<sup>1</sup>This final state is similar to the double milling states found in biological swarms [12]

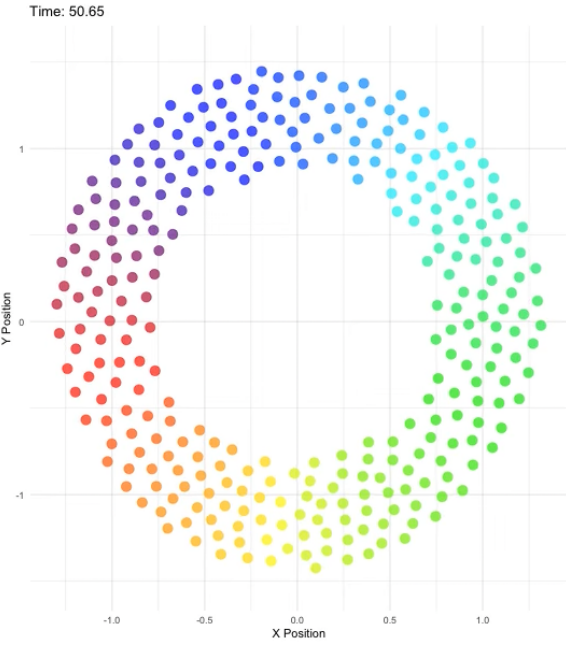
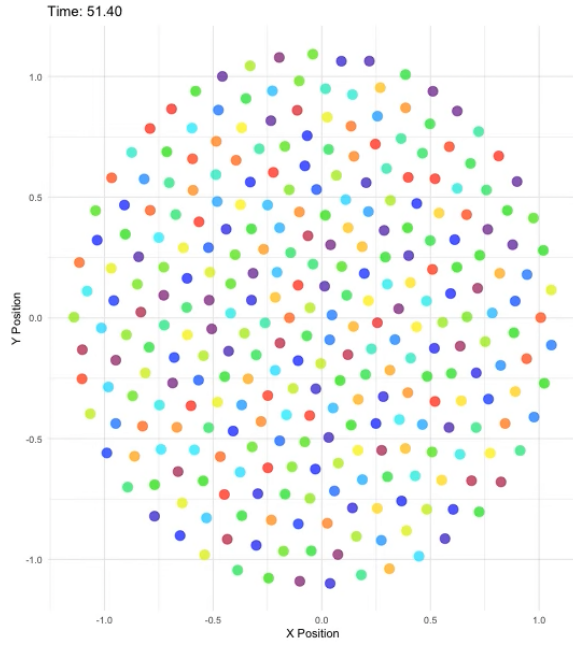


Figure 1.3: Static asynchronous state ( $K = -1, J = 0.1$ )

Figure 1.4: Static phase wave state ( $K = 0, J = 1$ )

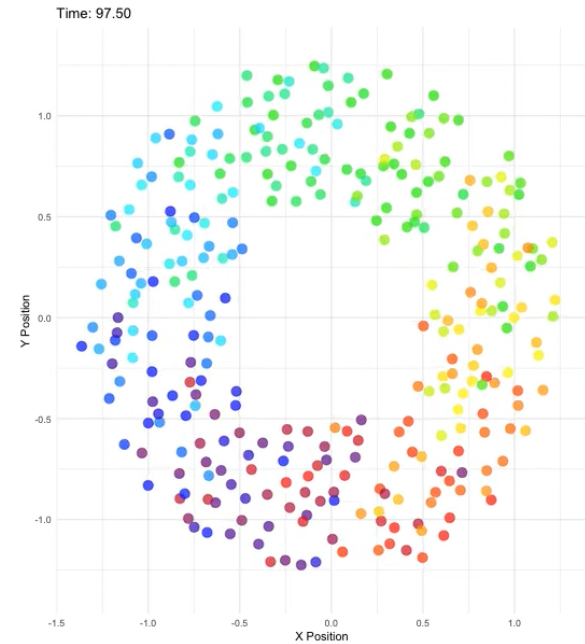
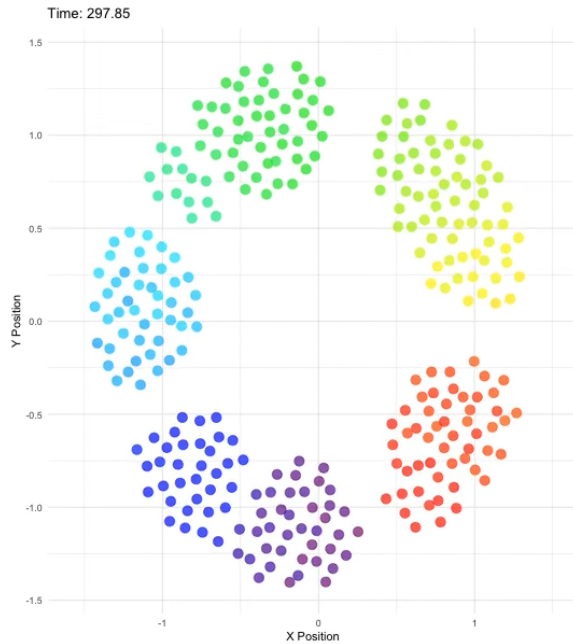


Figure 1.5: Splinter phase wave state ( $K = -0.1, J = 1$ )

Figure 1.6: Active phase wave state ( $K = -0.6, J = 0.9$ )

# Appendix: Swarmalators on an ER Network

---

We now explore how the active phase wave state ( $K = -0.6$ ,  $J = 0.9$ ) behaves on an Erdős-Rényi (ER) network as the connection probability  $p$  increases.

## 1.3 | Order Parameters

---

A useful way to assess the system's state is through three order parameters [9], independent of the network topology:

- $r$  measures the degree of phase synchronization, ranging from 0 (desynchronized) to 1 (fully synchronized), as introduced in the Kuramoto model [7]:

$$r = \left| \frac{1}{N} \sum_{j=1}^N e^{i\theta_j} \right| \quad (1.3)$$

- $S$  quantifies the correlation between phases  $\theta_j$  and spatial angles  $\phi_j$ :

$$S = \max \left\{ \left| \frac{1}{N} \sum_{j=1}^N e^{i(\phi_j + \theta_j)} \right|, \left| \frac{1}{N} \sum_{j=1}^N e^{i(\phi_j - \theta_j)} \right| \right\} \quad (1.4)$$

- $U$  measures the fraction of swarmalators that complete at least one full cycle in both space and phase:

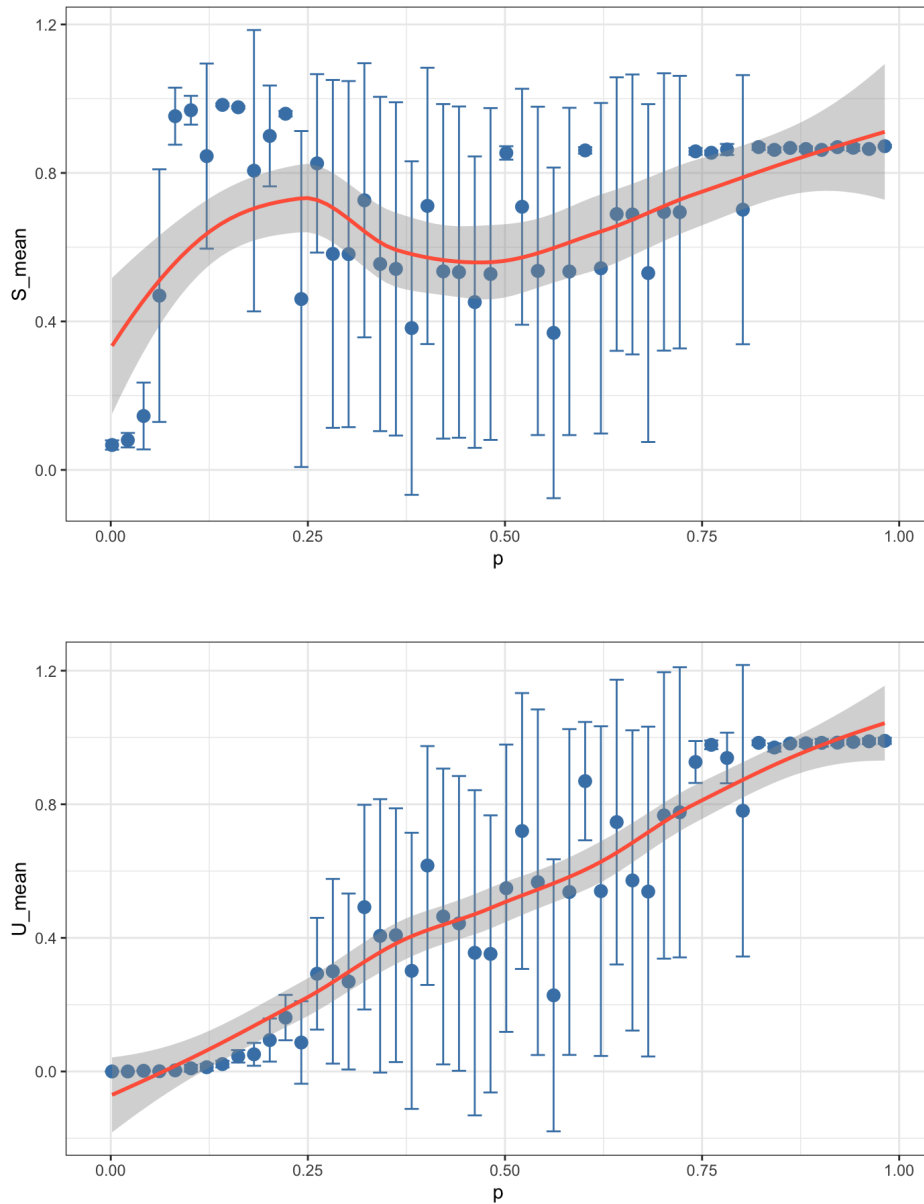
$$U = \frac{N_{rot}}{N} \quad (1.5)$$

$S$  is positive in both splintered and active phase wave states, while  $U$  is non-zero only in the active phase wave.

## 1.4 | ER Network

Using tools from the third laboratory, we implemented functions to compute the order parameters for each simulation. After reaching the steady state ( $t_f = 300$ ), we computed  $r$ ,  $S$  (discarding the transient dynamics), and  $U$ . Each value of  $p$  was averaged over five different realizations of the system to obtain means and standard deviations.

The results for  $S$  and  $U$  are shown below.



Due to the significant errors observed for intermediate values of  $p$  (likely a consequence of the limited simulation time, which could be greatly improved), only limited conclusions can be drawn regarding the functional forms of the order parameters. However, for both  $S$  and  $U$ , we can distinguish a region at low  $p$ , where the value is zero, and regions at higher  $p$  values, closer to 1, where the parameters seem to approach asymptotic values.

It is possible that, as connectivity increases, more swarmalators interact, leading to greater spatial-phase rotation and synchronization. For  $S$  this could also be related to the emergence of the giant connected component (GCC).

## 2 | Modelling language competition on a complex network

---

### 2.1 | Model presentation

---

Our global language heritage is at risk: about 50% of the 6,000 languages spoken today may face extinction this century. In this context, simple models describing language competition can offer useful insights for policy-making.

A dynamical analysis of different networks can clarify the interplay between language competition and social aggregation. Our analysis stems from the Abrams and Strogatz model, which explores endangered language dynamics [13]. Their study considers a two-state society, with speakers of **language A** or **language B**, and describes the system's evolution using an ODE to derive transition probabilities.

The model predicts that one language will eventually drive the other to extinction. However, since bilingual societies exist, the model requires refinement to account for this behavior.

Castelló et al. [14] examine agents on three types of networks: regular, small-world, and social [15]. They also introduce a bilingual state, **AB** (i.e., simultaneous use of both **A** and **B**)<sup>1</sup>.

In this setup, agent  $j$  sits on a network, of  $N$  individuals, with  $k_j$  neighbors. The state of an agent evolves as follows: at each iteration, we choose agent  $i$  at random and compute the local densities of language users in the neighborhood of agent  $i$ , denoted  $\sigma_i^l$  (where  $l \in \{\mathbf{A}, \mathbf{B}, \mathbf{AB}\}$  and  $\sigma_i^A + \sigma_i^B + \sigma_i^{AB} = 1$ ). Agent  $i$  changes state according to the following transition probabilities: <sup>2</sup> <sup>3</sup>.

$$\begin{aligned} p_{i,A \rightarrow AB} &= \frac{1}{2}\sigma_i^B & p_{i,B \rightarrow AB} &= \frac{1}{2}\sigma_i^A \\ p_{i,AB \rightarrow B} &= \frac{1}{2}(1 - \sigma_i^A) & p_{i,AB \rightarrow A} &= \frac{1}{2}(1 - \sigma_i^B) \end{aligned} \tag{2.1}$$

Finally, for each network, results are compared to an agent-based version of the Strogatz two-state model:

$$p_{i,A \rightarrow B} = \frac{1}{2}\sigma_i^B \quad p_{i,B \rightarrow A} = \frac{1}{2}\sigma_i^A \tag{2.2}$$

Our goal is to reproduce the results of Castelló et al. [14] for lattice and small-world networks.

<sup>1</sup>We always refer to language use rather than competence. Thus, a person can leave the bilingual state at any time.

<sup>2</sup>**A** and **B** have equal status: in fact eq (2.1) are symmetric under the exchange of A and B.

<sup>3</sup>Note that transitions between monolingual **A** and monolingual **B** always pass through the bilingual state.

## 2.2 | Two-dimensional regular network

In this lattice, each node has four neighbors under periodic boundary conditions (PBC). Each node  $i$  is assigned a vector component  $S_i$ , which can take one of three possible values, representing different states. The initial configuration is randomly drawn from a uniform distribution.

We primarily use *igraph* for network manipulation and *ggplot2* for plotting. To speed up computations, nodes fully embedded in a uniform domain (not at the boundary) are excluded from the evolution algorithm.

As observed by Castelló, domains of monolingual communities undergo coarsening, with larger domains growing at the expense of smaller ones, while bilingual agents form narrow bands between monolingual regions. The system eventually reaches a dominance-extinction state.

Similar behavior is found in the agent-based Abrams-Strogatz model. However coarsening here is slower and driven by interfacial noise. Below are two snapshots of the dynamics: red nodes are in state A, black in state B, and white in AB.



Figure 2.1: Bilingual,  $N = 625$ ,  $t = 0$

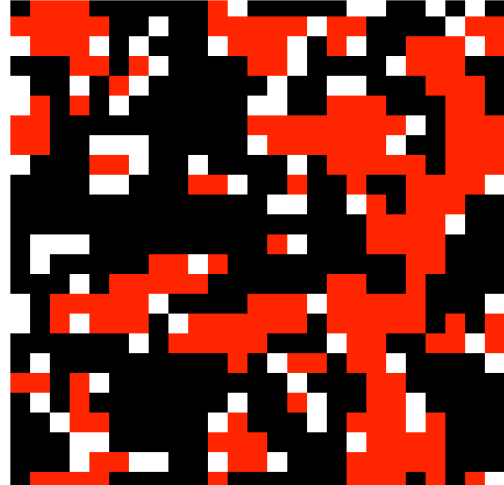


Figure 2.2: Bilingual,  $t = 5000$



Figure 2.3: A-S model,  $N = 625$ ,  $t = 0$

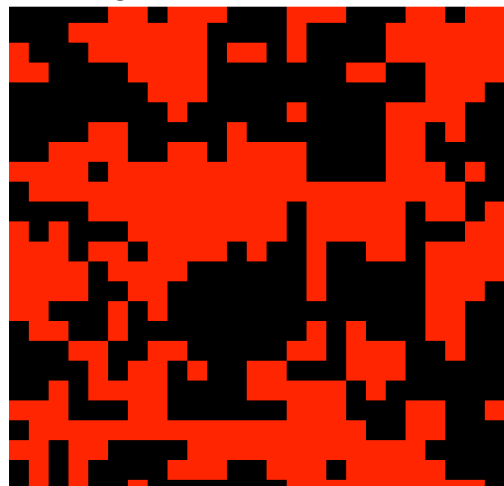


Figure 2.4: A-S model,  $t = 5000$

## 2.3 | Small-world Network

We study the dynamics on a two-dimensional small-world network to analyze the effect of long-range social interaction. We set  $p = 0.1$ .

In agreement with [14], we find that long-range interactions inhibit the formation and growth of domains, allowing for long-lived metastable states. However, the system will eventually settle into a dominance-extinction state. On the other hand, bilingual agents tend to destroy metastable states of dynamical coexistence and accelerate the decay toward the extinction of one of the languages, as noted by [16].

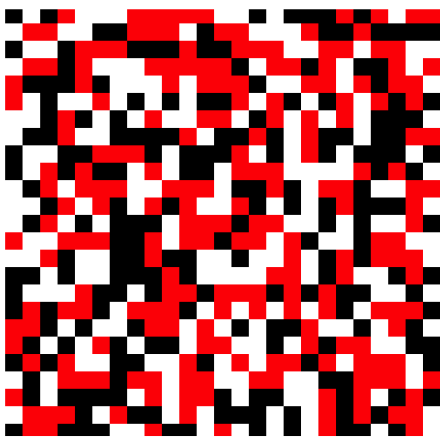


Figure 2.5: Bilingual,  $N = 625$ ,  $t = 0$

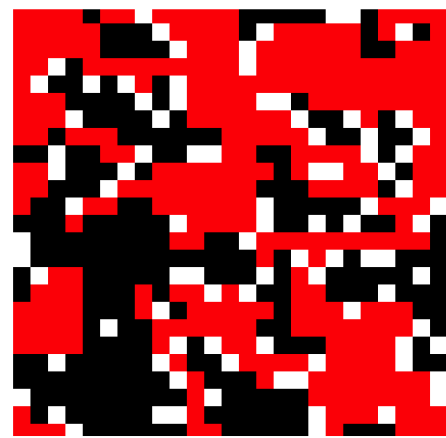


Figure 2.6: Bilingual,  $t = 5000$

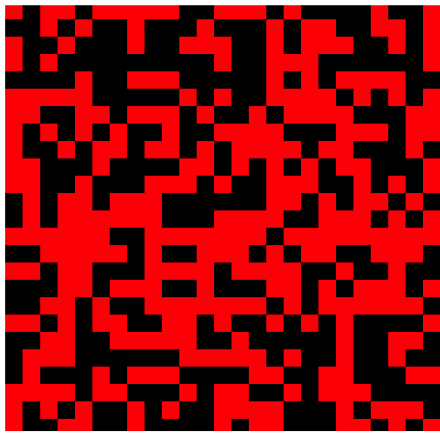


Figure 2.7: A-S model,  $N = 625$ ,  $t = 0$

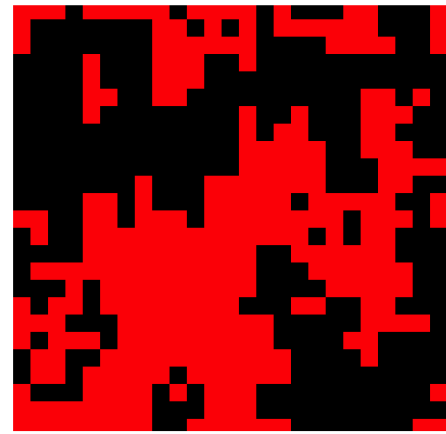


Figure 2.8: A-S model,  $t = 5000$

In conclusion AB-agents produce an essential modification of the processes of coarsening and domain growth, changing the interfacial noise dynamics of the agent based Strogatz model into a curvature driven interface dynamics.

However, in the topology considered, we haven't been able to reproduce stable bilingual coexistence. In fact it seems that bilingualism is not an efficient mechanism to stabilize language diversity when a social structure of interactions such as the small world network is taken into account. In contrast, bilingual agents are generally found to ease the approach, absorbing monolingual states by an obvious effect of smoothing the communication across linguistic borders.

# 3 | Social Connectedness Index I from Facebook

---

## 3.1 | Task Presentation

---

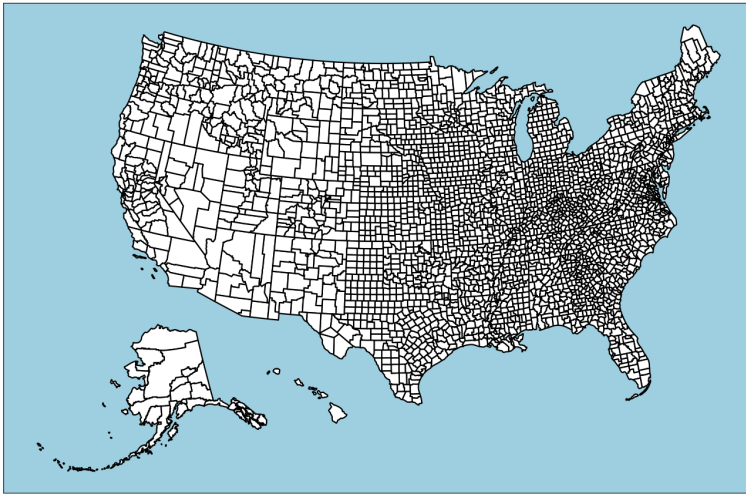


Figure 3.1: Map of U.S. counties (Alaska and Hawaii have been displaced for a more compact representation)

The task is to build a network for each U.S. state, where the nodes represent counties, based on a dataset describing social connectivity between different regions [17]. Each edge is characterized by a *Social Connectivity Index (sci)*.

This measure was first proposed and analyzed in [18].

Formally, the *sci* between two locations  $i$  and  $j$  is defined as:

$$sci_{i,j} = \frac{\text{FB Connections}_{i,j}}{\text{FB Users}_i \times \text{FB Users}_j} \quad (3.1)$$

where  $\text{FB Users}_i$  and  $\text{FB Users}_j$  are the numbers of Facebook users in locations  $i$  and  $j$ , respectively, and  $\text{FB Connections}_{i,j}$  is the total number of Facebook friendship connections between individuals in the two locations.

To protect individual privacy, the *sci* has been scaled between 1 and 1,000,000,000, with a small amount of noise added and the result rounded to the nearest integer.

The *sci* index can be interpreted as the **relative probability of a Facebook friendship** link between two users located in  $i$  and  $j$ . In other words, if this measure is twice as large, a user in  $i$  is twice as likely to be connected with a user in  $j$ .

The dataset provides edges, characterized by the columns: starting node (**user\_loc**), ending node (**fr\_loc**), and weight (**scaled\_sci**).

We consider the network as simple, ignoring friendships within each county.

## 3.2 | Data Handling

For this analysis, we used the *igraph* package for network manipulation, *ggplot2* for plotting, and *tigris* for retrieving county information. Figure 3.3 was generated using the *usmap* package.

The procedure was as follows: First, we imported a county dataset from *tigris* (from the year 2018 to match the county subdivisions in [18]), modified it (for example, by adding a column for county centroids used later for plotting), and split it by state. Then, we imported the *US counties-US counties sci* dataset from [17] and applied a similar procedure (removing edges between different states). Finally, we generated node and edge files for each state and plotted the corresponding networks.

Here is an example with California:

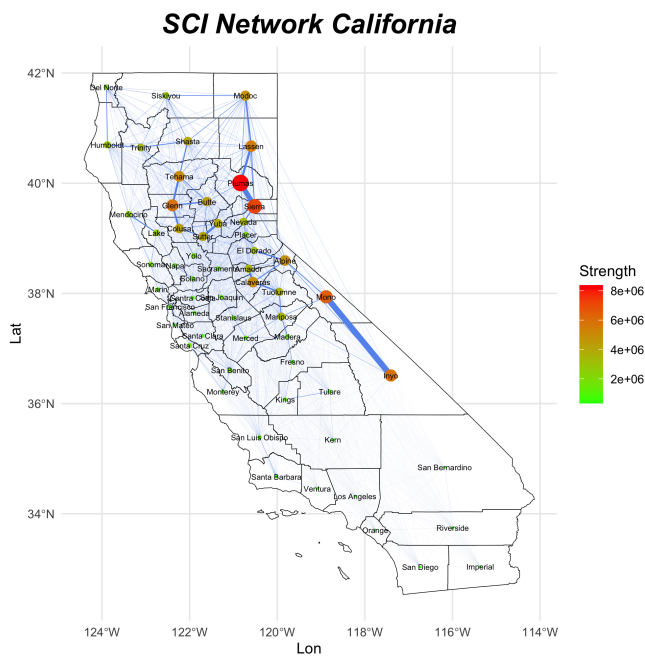


Figure 3.2: California sci network (node sizes and colors depend on their strengths, and edge widths are proportional to their weights.)

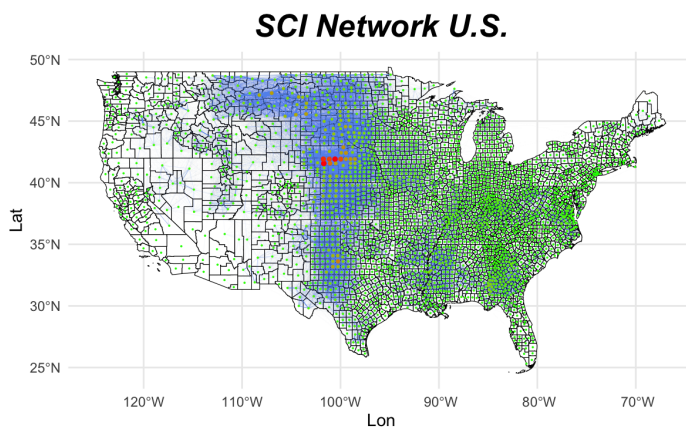


Figure 3.3: U.S. entire sci network (node sizes and colors depend on their strengths, and edge widths are proportional to their weights.).

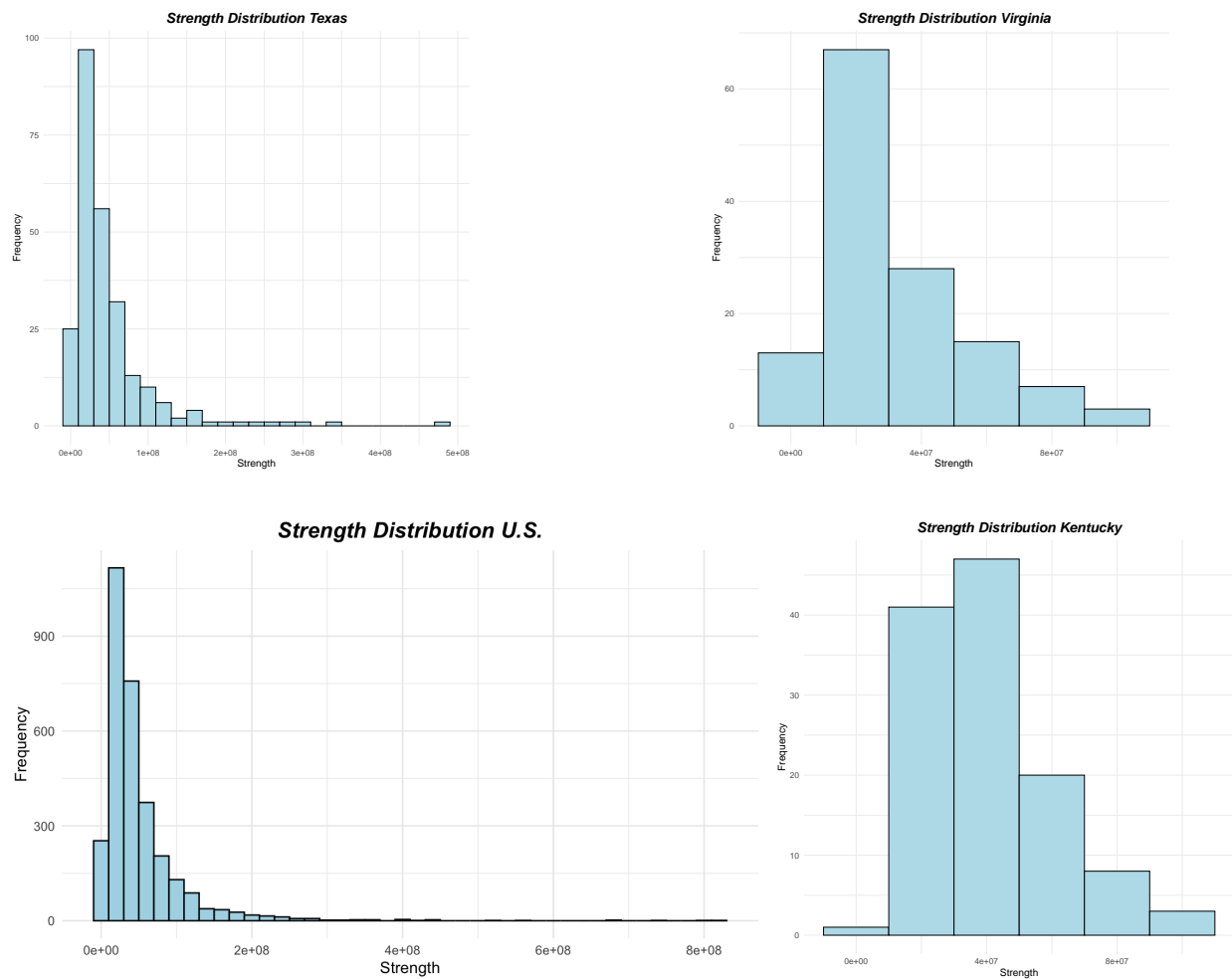
### 3.3 | Data Analytics

Regions with only one node were excluded from the analysis. Even with this criterion, network sizes vary significantly, from the *U.S. Virgin Islands* with just 3 nodes, to *Texas* with 254 nodes (the average is around 60 nodes).

Most networks are complete, except for *American Samoa*, *Hawaii*, and the *Northern Mariana Islands*—each with 5 or fewer nodes—making degree analysis uninformative. Since the networks are weighted, we focused on node strength, as shown in figure ??, and used SCI in the descriptors.

Interestingly, counties with the highest strength often have smaller populations. This may be because intra-county connections were ignored, and people in less populated areas tend to have more long-range friendships compared to those in denser regions.

We also generated histograms to analyze the strength distribution per state and across the U.S. While no clear patterns emerged from the frequency histograms, focusing on states with more than 100 counties (where statistical analysis is more reliable) reveals a consistent shape: an initial peak followed by a sharp decrease in frequency for higher strengths.



# Remarks

---

Part of the code was generated with the assistance of ChatGPT (v4); however, it was never used blindly.

For instance, this tool helped build functions for calculating the  $U$  order parameter, generating videos, plotting networks, and converting between degrees and DMS formats. Moreover, it suggested useful packages, such as *tigris*.

Finally, it was helpful in checking grammar and making minor adjustments to improve the readability of the text.

## 4 | Bibliography

---

- [1] James E. Martin and Alexey Snejhko. Driving self-assembly and emergent dynamics in colloidal suspensions by time-dependent magnetic fields. *Reports on Progress in Physics*, 76(12), 11 2013.
- [2] Alexey Snejhko and Igor S. Aranson. Magnetic manipulation of self-assembled colloidal asters. *Nature materials*, 10 9:698–703, 2011.
- [3] Jing Yan, Moses Bloom, Sung Chul Bae, Erik Luijten, and Steve Granick. Linking synchronization to self-assembly using magnetic janus colloids. *Nature*, 491:578–581, 2012.
- [4] O. A. Igoshin, A. Mogilner, R. D. Welch, D. Kaiser, and G. Oster. Pattern formation and traveling waves in myxobacteria: theory and modeling. *Proceedings of the National Academy of Sciences*, 98:14913–14918, 2001.
- [5] M. Iwasa, K. Iida, and D. Tanaka. Hierarchical cluster structures in a one-dimensional swarm oscillator model. *Physical Review E*, 81:046220, 2010.
- [6] D. Tanaka. General chemotactic model of oscillators. *Physical Review Letters*, 99:134103, 2007.
- [7] Juan Acebron, Luis Bonilla, Conrad Vicente, Felix Ritort, and Renato Spigler. The kuramoto model: A simple paradigm for synchronization phenomena. *Reviews of Modern Physics*, 77:137, 01 2005.
- [8] Francisco A. Rodrigues, Thomas K. DM. Peron, Peng Ji, and Jürgen Kurths. The kuramoto model in complex networks. *Physics Reports*, 610:1–98, January 2016.
- [9] Kevin P. O’Keeffe, Hyunsuk Hong, and Steven H. Strogatz. Oscillators that sync and swarm. *Nature Communications*, 8(1), November 2017.
- [10] Gourab Kumar Sar and Dibakar Ghosh. Dynamics of swarmalators: A pedagogical review. *Europhysics Letters*, 139(5):53001, August 2022.
- [11] Jeongho Kim Jinyeong Park Seung-Yeal Ha, Jinwook Jung and Xiongtao Zhang. Emergent behaviors of the swarmalator model for position-phase aggregation. *Mathematical Models and Methods in Applied Sciences*, 29(12):2225, 2019.
- [12] J. Carrillo, Maria R. D’Orsogna, and Vladislav Panferov. Double milling in self-propelled swarms from kinetic theory, preprint uab. *Kinet. Relat. Models*, 2:363–378, 06 2009.
- [13] Daniel Abrams and Steven Strogatz. Linguistics - modelling the dynamics of language death. *Nature*, 424:900, 09 2003.

- [14] Xavier Castelló, Víctor Eguíluz, Maxi Miguel, Lucia Loureiro-Porto, Riitta Toivonen, Jari Saramäki, and Kimmo Kaski. Modelling language competition: bilingualism and complex social networks. 05 2008.
- [15] Riitta Toivonen, Jukka-Pekka Onnela, Jari Saramäki, Jörkki Hyvönen, and Kimmo Kaski. A model for social networks. *Physica A: Statistical Mechanics and its Applications*, 371(2):851–860, 2006.
- [16] Xavier Castelló, Víctor M Eguíluz, and Maxi San Miguel. Ordering dynamics with two non-excluding options: bilingualism in language competition. *New Journal of Physics*, 8(12):308–308, December 2006.
- [17] Fb social connectedness index. <https://data.humdata.org/dataset/social-connectedness-index>. [Modified: 13 October 2021].
- [18] Michael Bailey, Rachel Cao, Theresa Kuchler, Johannes Stroebel, and Arlene Wong. Social connectdness: Measurement, determinants, and effects. *Journal of Economic Perspectives*, 32(3):259–80, 2018.